GEOMETRIC CONSIDERATIONS OF PLASTICITY IN STRUCTURAL CONCRETE ANALYSIS AND DESIGN

John EYRE

Department of Civil and Environmental Engineering, UCL

Keywords: yield criteria, graphical visualisation, upper bounds, concrete slabs and beams, membrane action, plane stress, design tools.

1 INTRODUCTION

The shift, provoked perhaps by a world war involving air raids, away from a linear elastic idealisation of material performance in structural analytical methods to one of perfect plasticity inspired research in many countries but the pioneering research in Cambridge and Copenhagen continues to stand out as a landmark. Such methods have been embraced by the designer for reasons of simplicity and verisimilitude when the strength and safety of a structure is the issue. With the introduction of plasticity the mathematical modelling of a postulated structure became free of the need to satisfy simultaneously both statical and kinematical laws. Although an approximation, plasticity provided information hitherto unavailable on behaviour and load paths at and near collapse. The methods were attractive and, despite the natural conservatism within the profession, they became the unquestioned norm for strength calculations in structures.

Furthermore, the methods of plasticity are very much more akin to the thinking patterns of a designer. Designers have the inescapable responsibility of anticipating every possible mode of failure. This includes consideration of appropriateness and suitability for intended use, the implications of manufacture, visual suitability and environmental responsibility and fitness for the structural life; all being commensurate with economic resource and value. The power of imagination applied to the visualisation of collapse mechanisms is an intimate part of the designer's cerebral equipment.

Graphical methods have always been a useful tool for the designer and the recognition of scale and proportion enables engineers not only to make appropriate assessments on stress magnitudes but also to assess whether or not the results they receive from a computer are within the right area. Historically graphics were used with appropriate precision for the modelling of vectors in for example member force identification in pin-jointed frameworks (Clarke-Maxwell's reciprocal diagrams) and their deflections (Williot/Mohr). They were also used for tensor transformations (Mohr) of stress and strain. New ideas in graphics continue with the example of Magnell's presentation of a solution space for the section design in prestressed concrete which has recently been recalibrated for the convenient use of the designer (Calladine [1]).

As soon as yield involves a plurality of simultaneous stress states then a yield criterion becomes a geometric surface in the space of these stress states. Planes through such surfaces may provide useful practical information, in a visually acceptable two dimensional format, on the performance of structures using a language with which the designer is innately familiar.

Chris Morley has been at the focus of the use of yield criteria in better understanding the behaviour of the elements of reinforced concrete structures. This paper considers two areas of his interest: membrane action in the yield line analysis of slabs; and shear failure of beams. It reflects in particular on how visualisation of the yield criterion geometry provides information for intuitive use by the designer.

2 MEMBRANE ACTION IN REINFORCED CONCRETE SLABS

Membrane action in concrete slabs is a favourite field among researchers. This interest reflects the well recognised existence of slab strengths in excess of those both calculable by convenient design methods and demonstrable where required in 'job calculations'. In addition to the lack of knowledge available to the designer on the magnitudes and effects of slab boundary restraints, giving rise to membrane enhanced strengths, the complexity of analysis and remoteness of the phenomenon allows only a very limited intuitive understanding. This affects confidence and strongly inhibits the use of membrane action in routine calculations. The researcher then needs to address the

conceptualisation issue as much as completing the knowledge base. Since it will be required in any enhancement in slab strength, the yield condition of structural element sections under bending moment and membrane force is considered first.

2.1 The yield criterion

Combined stress resultants on the mid-plane of a yielding section of a Tresca plate are shown inset in Figure 1(a). (It is convenient in this paper to consider compressive aspects positive and to show compression abscissae to the left of the origin. Positive "sagging" bending moment ordinates shall be shown above the origin.) The presence of a second stress resultant never improves the capacity of the yielding section in respect of the first (maximum and minimum occur under pure bending moment or pure in-plane stress). When membrane action is invoked by a mechanism, strength gain is a second order geometric effect with increasing significance at rather advanced deflections. The material assumption for the reinforcement in a concrete slab may also be that of a Tresca solid, but the concrete is assumed to be rigid-plastic in compression at a prescribed yield value (f_c) and to crack immediately on tensile straining ($\varepsilon = 0,\ d\varepsilon \le 0, f_t = 0$). In these circumstances the yield criterion for a section with a reference at the level of the reinforcement is shown in Figure 1(b). In this case the pure stress resultants can be improved upon by combination with a second and a mechanism with invoked membrane action in a slab provides considerable extra strength as a first order effect in the mechanism's early progress. The yield criterion using the conventional mid-depth position has been shown before (e.g. Janas [2] and Braestrup [3]). Moving the point of reference from the reinforcement level to mid-depth produces a "rotation" of the yield criterion (an apparent rotation produced by rescaling the ordinates only) and the figure becomes antisymmetric. The range of practical significance lies between point J and the maximum positive moment at point H.

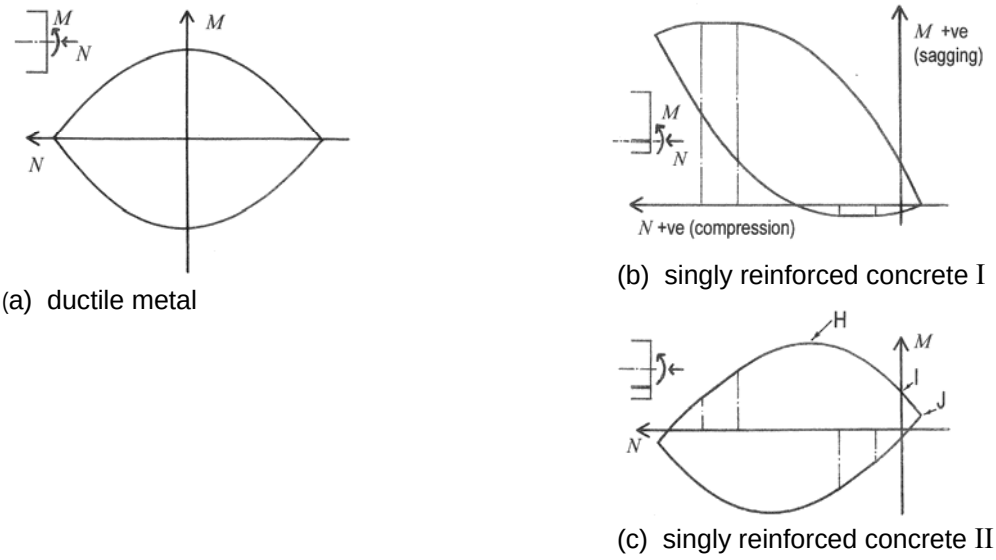

(a) ductile metal

(b) singly reinforced concrete I

(c) singly reinforced concrete II

Fig. 1 Criteria for yielding lines of plate elements under bending moment and membrane stress resultants.

2.2 The load-improvement – deflection relationship

In 1967 Morley [4] implicitly made use of this region of the criterion in a rigid-plastic analysis of a regular polygonal slab, isotropically reinforced with symmetric hogging and sagging tension reinforcement. A slab, rigidly restrained at its perimeter and subject to a transverse load, was shown to have a load-improvement deflection relationship of

$$p = 1 + \frac{\alpha^2}{4\beta} - \frac{\alpha}{2}\delta + \frac{5\beta}{12}\delta^2 \qquad (1)$$

Soon afterwards Janas [2] provided the equation for the one-way spanning strip with surface reinforcement but subsequently in Reference [5] refined the equation to

$$p = 1 + \frac{\alpha^2}{4\beta} - \alpha\delta + \beta\delta^2 \qquad (2)$$

Equation 2 is a generalised form of Janas' surface reinforced 'sandwich' slab to allow for a free choice of cover thickness to the reinforcement.

In the above equations the load p is the normalised load $p = P/P_y$ where P_y is the yield line theory upper bound load using pure moment slab properties, α and β are parameters defining the section as follows: α is the ratio of the neutral axis level above section mid-depth to the lever arm and β is the ratio of the depth to the centroid of compression to the lever arm both during yield in pure flexure. The deflection at its geometric maximum is w_o but is expressed non-dimensionally here as $\delta=((\alpha/2\beta)+1)(w_o/h)$ where h is the slab thickness.

The above Equations 1 and 2 appear in a different form from the originals to use a non-dimensionalization based on the stress block parameters α and β devised by Wood [6] in his formulation of the yield criterion shown in Figure 2(a). The restrained one-way strip load-improvement deflection relationship, Equation 2, is shown in Figure 2(b). The load curve is shown over its entire range of validity. At zero deflection yield commences with the neutral axes at section mid-depth at the slab restraints and in the span. Unloading takes place with deflection until (at pure flexure load) the neutral axes are all at their pure flexure levels within the section and the graph terminates at the point where the neutral axes coincide with the slab surface producing full depth cracks.

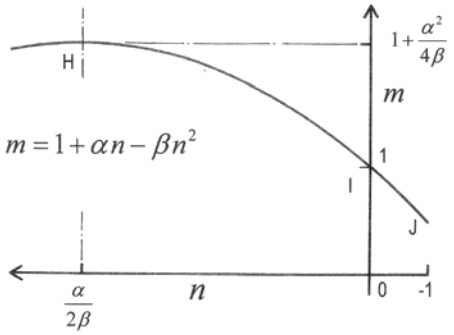

(a) Wood's yield criterion [6]

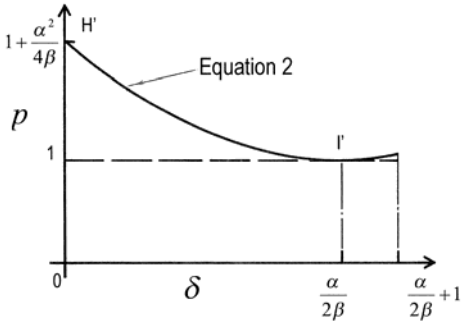

(b) Load-deflection curve for a rigidly restrained one-way slab (Janas [2]).

Fig. 2 Yield criterion and load curves compared

The non-dimensional bending moment m is the ratio of the moment capacity under membrane force to the pure flexure yield moment and the membrane force n is expressed as a multiple of the tensile yield force in the reinforcement per unit length of yield line.

The geometric similarity of these two curves was reported by Eyre & Kemp in 1983 [7]. The horizontal spacing of the points H, I and J of Fig 2 (a) is also that of points H', I' and the end of the curve of Figure 2(b) and the ordinates of H & I are the same as H' and I'. Reference [7] showed that when the two curves are superimposed the load-improvement – deflection curve is a simple 'reflection' about a line joining points H & I. Figure 3(b) shows this graphical construction. The word 'reflection' refers to the ordinates only of the two curves illustrated by the dimensions 'y' shown on the graph. At point H the improvement in the load and that of the bending moment have the same value and at this point the membrane force is at a maximum, Fig 3(a), and the neutral axis is at mid-depth. At the other point common to both curves, point I, membrane force is zero and the neutral axis is at its pure flexure level. The limit of this pattern of yield is achieved when the neutral axis is at the slab top surface. Further to the description given in Reference [7], Figure 3 shows that this set of curves may be fitted to the section half depth and the line X-X traces the neutral axis position in all yielding sections during yield.

The illustration that the load curve can be generated in this way is a valuable reminder that only the properties of the section affect the load-improvement. The load expressed in this way is independent of span-depth ratio, of load distribution and of assumed mechanism.

This construction applies to the special case of a slab reinforced with equal amounts of tension reinforcement at the support and within the span, so that $\gamma = 1$ where γ is the ratio of the reinforcement area at the support to that at the span. For the general case Janas' equation may be shown to be

$$p = 1 + \frac{2\beta}{1+\gamma_1}(\alpha_1^{\,2} - 2\alpha_1\delta + \delta^2) \tag{3}$$

where $\alpha_1 = (\alpha/\beta + 1 - \gamma)/2$ and γ_1 is the ratio of the pure flexure yield moment at the support to that at the span. The load curve construction procedure may be extended to cover the case of unequal reinforcement intensities as shown in Figure 4. In this figure the curve for p' is for the case of $\gamma = 1.0$. The axis for the required load-improvement (p) in the case of any other value of γ is plotted in a new position a distance $(1-\gamma)/2$ to the left of the original axis (p') and a new curve is plotted by scaling the ordinates such that

$$\frac{TS}{TQ} = \frac{2}{1+\gamma_1} \tag{4}$$

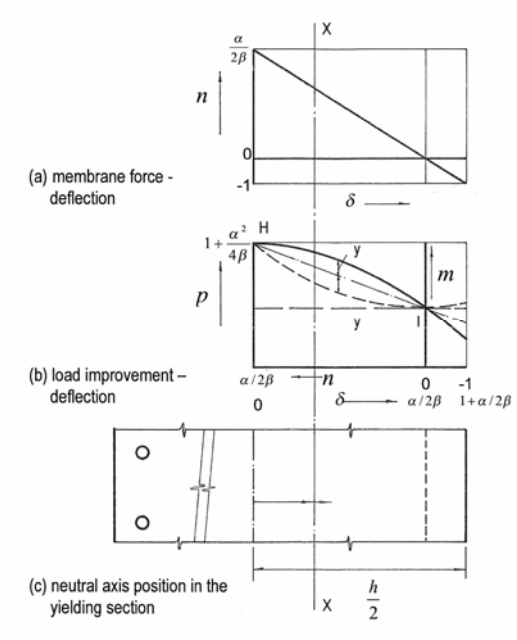

Fig. 3 Graphical construction of the load-deflection curve

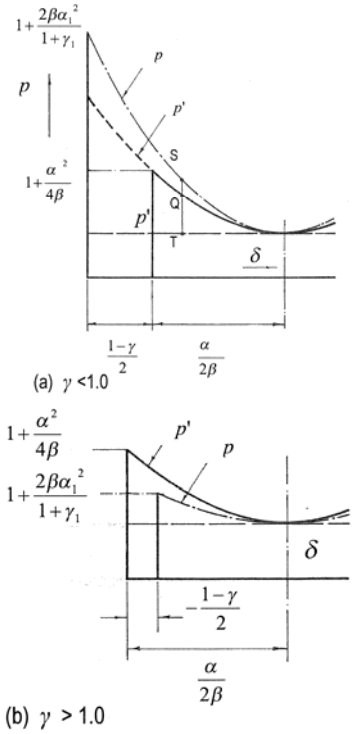

Fig. 4 The load curve for any γ

It is therefore possible to construct the rigid-plastic load-deflection curve for any one-way spanning reinforced concrete slab. These constructions may be used to visualize the effect of variations in the section parameters.

2.3 Variations in section parameters

The non-dimensional description of the reinforced concrete section requires two quantities. Wood's selection of α and β were simply transformations of the more readily appreciated Φ and h/d (in Morley's case 2Φ and h/d), where $\Phi = 0.5A_s f_y/(df_c)$ and d is the effective depth of the tension reinforcement. Any variation of the reinforcement intensity expressed as Φ can be visualized by determining the pure flexure neutral axis position. In reference [7] this has been illustrated by showing separate graphs for different reinforcement areas using the more practical deflection parameter w_o/h. The deflection δ is proposed as a more convenient form for analysis and used here showing the different curves superimposed (Fig. 5). The section half depth is used to define the complete deflection range and a parabola is drawn with its maximum at mid-depth within an enclosing rectangle defined by points H and J.

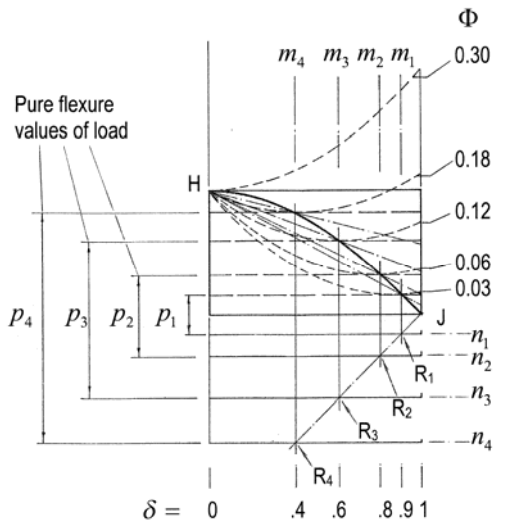

Fig. 5 Load-improvement for a range of Φ (constant h/d)

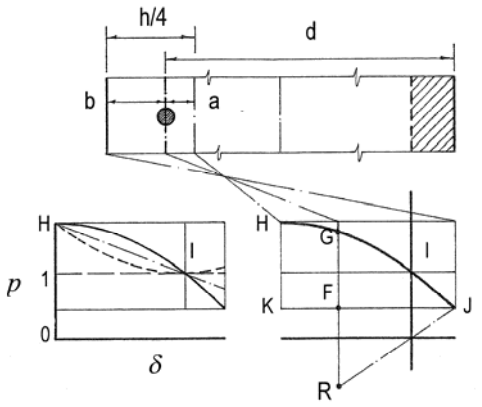

Fig. 6 The complete criterion construction from section parameters

Five reinforcement intensities are shown and four of the cases are identified with a suffix where needed. In each case the m axis is defined by the pure flexure neutral axis depth. The load-improvement curves shown as broken lines are determined using the reflection lines in each case. This provides a visualization of the effect of reinforcement intensity on load improvement. It is known that lightly reinforced sections offer a greater potential for strength gain but this representation gives an impression of how much and the nature of the variation. It is illustrated here that when sufficient tension reinforcement is provided to produce a pure flexure neutral axis at mid-depth the resulting load curve shows no immediate improvement only a gradual increase in load capacity resulting from tension membrane action. This is precisely the type of response for the ductile metal (Tresca) case.

Missing from the description so far is the identification of the positions of the origins on the vertical axes. It may also be observed that so far only one of the section quantities, Φ, has been used. Different results may be furnished by different cover thicknesses provided to the reinforcement (i.e. different h/d). The horizontal axes drawn on Fig. 5 intersect with the m axes at points R_1, R_2 etc. and all points R_i lie on a common straight line through the yield criterion's extreme point J. The slope of the line through J may be determined in advance using the parameter h/d . Fig. 6 shows the identification of point R. R is plotted such that RF = FG on a vertical line positioned according to the depth of reinforcement within the section, making KF:FJ = a:b.

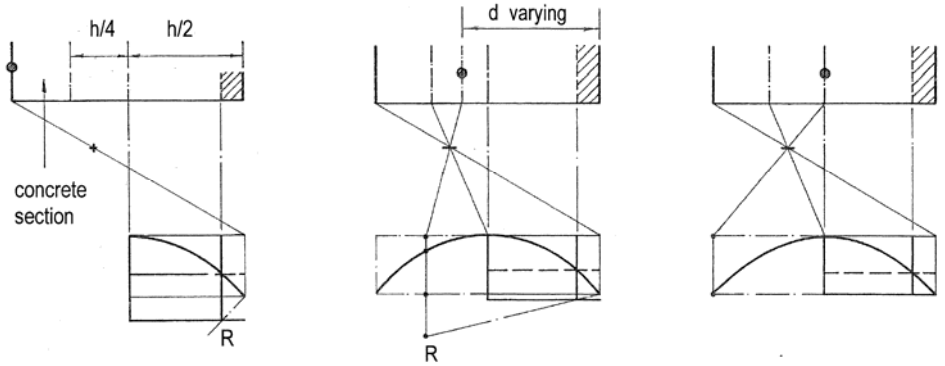

Fig. 7 The effect of variations in the cover parameter d/h

The effect of a wider variation of the cover parameter is shown in Fig. 7. As the depth to reinforcement (d) is reduced the load improvement p is increased. The load capacity (P) however is reduced due to the falling pure flexure load (P_y). The figure shows the full range between the limits to practical cases.

The algebraic/numerical calculation of the load curve depends upon the calculation of numerical values for the parameters α and β, however a complete construction can be made graphically from the familiar reinforced concrete section properties of pure flexure neutral axis depth and cover to reinforcement. The stages may briefly be summarized:

(i) on a parabola whose horizontal length represents the concrete half depth the m axis is plotted at the pure flexure neutral axis depth (Φ dependent).

(ii) the point R is identified noting the level of the reinforcement relative to the bottom quarter of the section (h/d dependent) and the n axis is drawn

(iii) the load curve is drawn using the reflection axis HI.

A fairly lengthy explanation was required to illustrate this construction. This procedure is not necessarily being offered for use in practice, although it is imagined that there are engineers in practice who enjoy determining magnitudes by graphical means. The knowledge of this construction helps, through visualization, to have an intuitive conception of what potential capabilities exist in a slab and of the effect of variations in section design. These are valuable notions for the designer long before attempts are made to put numerical calculations against the ideas.

However the designer will be concerned with slabs in which elastic strains in the slab and supports together with shrinkage combine to reduce the strength below this rigid-plastic estimate. Figure 8 shows the effect of different lateral elastic stiffnesses of a surround and different in-plane stiffnesses of the slab upon the load-deflection curves for real slabs.

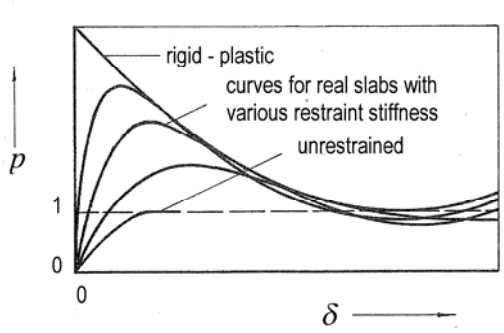

Fig. 8 The effect of elastic strains

In these circumstances membrane action varies with increasing magnitude during the early stages of yield. The motion along the yield criterion is toward the left on Fig.2(a) and the neutral axes move to reduce the length of the crack and introduce fresh concrete into the stress block. Now the techniques utilizing a strain rate definition of the resultant strain vector and of the neutral axis become inappropriate and equations developed by Wood [6] and Kemp [8] (elemental method) and Park [9] (strip method) for two way slabs and Christiansen [10] and Roberts [11] for the elastically restrained one-way strip are valid.

All the curves of Fig. 8 vary between the limits shown for infinite and zero stiffness. The rigid-plastic strain-rate curve therefore provides an envelope for the real load-deflection performance and is therefore an immediate guide to the way in which the section parameters of pure flexure neutral axis depth and cover will affect the load improvement due to membrane action.

3 SHEAR STRESS ANALYSIS

Rajendran & Morley [12], Bræstrup [13] and Neilsen & Bræstrup [14] have made important contributions to the plastic analysis of shear in plain and reinforced concrete structures. This was somewhat adventurous as concrete failing under shear does not behave in the ductile manner of lightly reinforced concrete slabs in bending nor does concrete actually fail in shear. Under normal practical circumstances the material concrete subjected to either shear or compression fails in tensile strain. Despite these two properties, the plastic analysis offered by the researchers into shear has provided valuable practical guidance and the geometric consequences of using different 'yield' criteria will be illustrated here.

3.1 Combined shear and compression in a defined line of weakness in a plane element

An analysis has been provided by Jensen [15] of the joint in a slant shear test specimen using a plane strain consideration. The subsequent plane stress modelling, Reference[16], provided an alternative view and is summarized here. The slant shear test is a compression test on a laboratory prism made in two halves with a joint (plane of weakness) arranged at an angle to the direction of the applied load as shown in Fig. 9(a). This exercise may be accepted as an analysis of a plane concrete material failing with a membrane yield line at an arbitrarily chosen angle within a monolithic material.

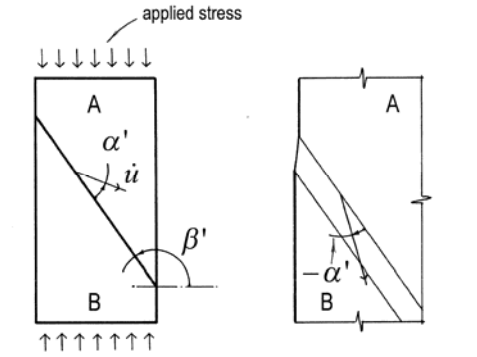

(a) the prism (b) an enlargement of the plastic zone

Fig. 9 The slant shear test

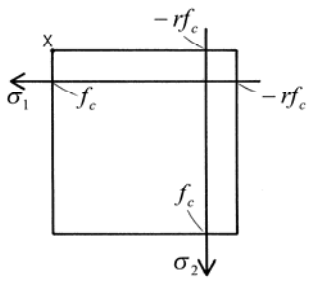

Fig. 10 The square yield criterion

Assuming that plastic flow takes place at the joint, a yield criterion may be chosen which would be a property of the joint and not necessarily of the materials of either of the two prism halves. The vector $\dot{u}$,shown at an arbitrary angle α' to the joint (positive anticlockwise), has the two components: shear along the joint and direct strain rate normal to the joint. The direct strain rate tangential to the joint is zero and therefore the principal strains will be of opposite sign (compression and tension) both functions of the direction α'. Fig. 9(b) shows the treatment of the joint and as the yield proceeds the vector $\dot{u}$ represents the velocity of half A relative to half B. Two different yield criteria were considered in Ref [16] both of which approximate observed results from tests on standard monolithic specimens. These are the square yield criterion and the plastic use of the Coulomb failure condition.

3.2 The square yield criterion

If yield is deemed to occur when a direct stress limit is reached then the criterion may be drawn in the two-dimensional principal direct stress space as shown in Fig. 10. The convention of compression positive is continued and is drawn positive downwards and to the left of the origin. The material in this case has a compressive yield stress of f_c and a ratio of tensile to compressive yield stress of r expressed as a positive value. Nielsen's consideration of a line in a monolithic material used $r = 0$.

The stress state during yield comprising both tensile and compressive flow indicates that the system is operating at point X on the criterion (Fig. 10). The equation of externally applied power to the rate of internal dissipation provides the applied loading in terms of the vector direction α' and a stationary value of load furnishes the unfortunately implicit expression for the direction α'.

$$\cos(\alpha'+\beta') = -\frac{1-r}{1+r}\sin\beta' \qquad (5)$$

Where β' is the joint line inclination shown in Fig. 9(a). A further algebraic step provides the least upper bound load, producing behavioural patterns depending on r as shown in Fig. 11.

The curious inquirer may want to know the vector directions (e.g. is there a component to the left or the right?, is it pure shear strain or is there a volume change in the plastic material?) and Equation 5 is far from satisfactory in this regard. The result, however, may be visualized if the representation of Fig. 12(a) is used. Borrowing from Mohr a semicircle of horizontal diameter $1+r$ is drawn with an origin at unit distance from the left-hand end. If the inclination of the yield line is superimposed and drawn through the origin the outward normal to the semicircle at its intersection with the superimposed line is at the required angle to the vertical. The angle α' on Fig. 12 is clockwise positive.

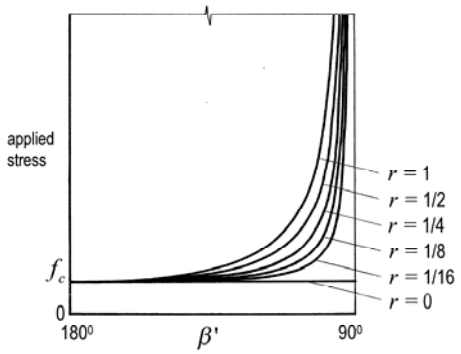

Fig. 11 Applied stress at yield for different joint angles

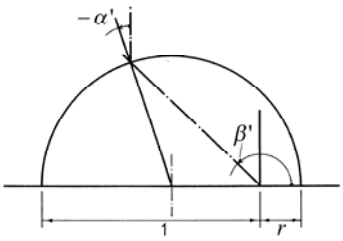

(a) Geometrical construction of the of the vector direction

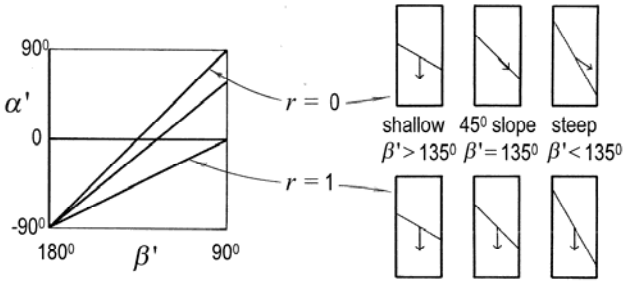

(b) visualisation for special cases of r

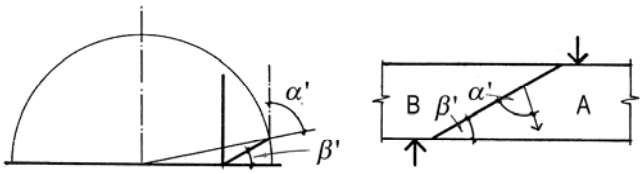

(c) motion of the plain concrete beam mechanism

Fig. 12 Flow vector visualisation

Although the idea for this came from the normality rule for strains drawn on a yield surface care should be taken not to consider the diagram as a yield criterion. The diagram at the moment can only be taken as the geometric expression of Equation 5. Fig. 12(b) demonstrates the results of Equation 5 showing the extremes of r = 1 and r = 0 and this may be readily observed from the semicircular representation.

For values of $\beta' \leq 90^0$ the construction may be used to visualize shear in a monolithic beam of this material Fig. 12 (c). The angle β' is determined by the length of the shear span and for this case of r<1 the value of α' is $\alpha' > (90^0 - \beta')$ providing a resultant lengthening of the beam. For r >1 the beam shortens and at r =1 there is no change in length during yield.

3.3 The modified Coulomb criterion

Reference [16] considers a second approximation of concrete material performance at failure, that of yield either (a) when Coulomb's failure criterion is met

$$|\tau| = \sigma_n \tan\phi + c \tag{6}$$

where the shearing resistance, τ , of a surface is dependent upon a normal stress, σ_n , acting on that surface and $\tan\phi$ and c define the gradient and intercept on the shear stress axis, or (b) when a direct tensile yield stress (f_t) is achieved. The definition is shown in shear and normal stress space in Fig. 13(a). The locus of yield conditions in plane stress is shown in Fig. 13(b). A more detailed

examination of the representation of Figs. 13(a) and 13(b) is provided in Reference 16. Fig. 13(a) may be used in the way of Fig. 12(a).

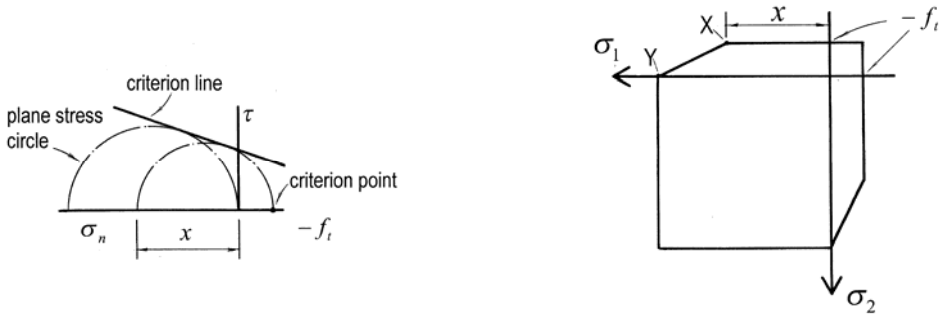

(a) the criterion drawn in shear / direct stress space (b) interpretation in 2-D principal stress space

Fig. 13 The modified Coulomb criterion

By superposition of the yield line at its given inclination to the horizontal axis the vector of plastic flow is given by the direction of the outward normal, Fig. 14. The resultant loading at yield may be seen in Reference 16.

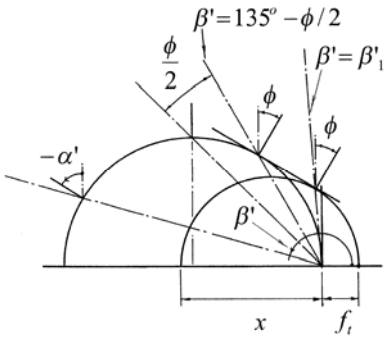

Fig. 14 Geometric presentation of vector directions

Of current interest is the yield geometry for different inclinations, β', of the yield line and this may now be traced visually. For high inclinations $\beta' \leq 135^0 - \varphi/2$ yield takes place in plane strain with $\alpha' = \varphi$ for the range $(135^0 - \varphi/2) \geq \beta' \geq \beta'_1$. As the inclination varies from a slope of $\beta \geq 135^0 - \varphi/2$ to the horizontal position the vector apparently changes from $\alpha' = \varphi$ through to $\alpha' = 0$ at $\beta' = 135^0$ and on to $\alpha' = -90^0$ at $\beta' = 135^0$. However on Figure 14 the semicircle is only a representation of stresses on axes of changing orientation and not a statement of the yield conditions. Within this range ($\beta \geq 135^0 - \varphi/2$) the material is yielding in shear at φ on the criterion but no longer confined to the σ_1, σ_2 plane. Under these circumstances yield takes place out of plane. For example for $\beta' \geq 135^0$ the vectors suggest a positive compressive strain rate and therefore a volumetric reduction. However the condition controlling yield is Coulomb's shear line with an associated dilation. The full 3-dimensional consideration is required in which a plane stress condition allows out-of-plane strains.

As with the discussion of the graphical representation of membrane action in slabs the value of graphics is in the intuitive understanding of the performance of elements at yield. This has greater value when considering shear in beams.

3.4 Longitudinally reinforced concrete beams

Neilsen and Bræstrup [14] provided the matching upper and lower bound solutions for the shear strength of a reinforced concrete beam, devoid of shear reinforcement. The concrete was assumed to be rigid-perfectly plastic with a square yield criterion defined by a compressive yield stress at some factor of the laboratory compressive strength (providing a value for f_c) and zero tensile strength ($r = 0$). The longitudinal reinforcement intensity was expressed as a ratio of the tensile yield force in both top and bottom layers of reinforcement to the compressive yield force of the gross concrete section. Using f_c in lieu of Neilsen's use of the compressive test strength (f_{cu}) the reinforcement intensity may be expressed as

$$\Phi' = \frac{f_y (A_s + A'_s)}{f_c bh} \tag{7}$$

where, for the reinforcement, f_y , A_s and A_s' are the yield stress and cross sectional areas of bottom and top layers respectively and b is the width of the beam. The beam mechanism is that of Fig 12(c) and the upper bound assumes full plasticity in the concrete along the diagonal line at β' to the beam's longitudinal axis and in direct tension in all layers of reinforcement in their longitudinal direction (no dowel action). The equation of virtual work rate provided the magnitude of the upper bound load in terms of the vector direction α' and minimising with respect to α' provided the solution

$$\cos(\alpha' + \beta') = -(1 - 2\Phi')\sin\beta \tag{8}$$

The solution is very similar to the plain concrete case of Equation 5 and equally inconvenient. However the graphical interpretation is just as satisfactory and shown in Figure 15. In this case a circle of unit diameter is used and the reinforcement intensity is marked thereon from the right hand end as a fraction of the diameter. In this case there is a visual display of the relative velocities of the mechanism which depends singly on the reinforcement intensity. The diagram shows the case of $\Phi' < 0.5$ in which case $\alpha' > 90^0 - \beta'$ resulting in a lengthening of the beam during yield, for $\Phi' > 0.5$ the beam shortens and the reinforcement is in compression and at $\Phi' = 0.5$ there is no length change and no effect on the reinforcement during progress of the mechanism.

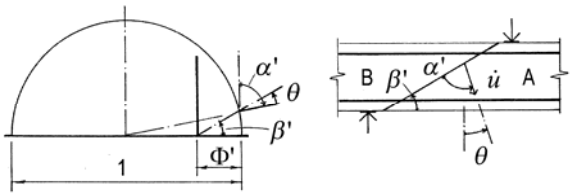

Fig. 15 Geometric construction for the longitudinally reinforced concrete beam

It should be noted that this historical snap-shot predates further work involving rotations in the elements of the mechanism and non-straight yield lines in the shear span carried on by Müller [17], Marti [18], Jensen [19] and Kemp & Al-Safi [20]. Such work refines the magnitude of the upper bound solutions in special cases. However the mechanisms arising from the described straight yield line and translational displacements allow this conceptual grasp of velocity and a guide to the likely benefits arising from beam end restraint.

4 DISCUSSION

Two distinct areas of the application of plasticity to reinforced concrete elements have been considered: the collapse of slabs into flexural yield line mechanisms under membrane force and bending moment; and "shear" failure in elements under plane stress. In both cases information is gained from the graphical display of the yield conditions and a superposition of a geometrical condition easily inferred from the failing structural system. The information provided may not be complete. For example these considerations are not a complete substitute for the use of calculation but, when considering the mental processes involved in the work of the designer, such a goal may not be of importance. It is however important to identify the limitations in what has been presented.

In the case of membrane action in slabs the graphical analysis described in this paper provides no information on kinematics. The focus is on variations in load capacity and the responsibility for identifying minimum load collapse mechanisms remains with the designer and the power of the imagination. The results given here for load, p, are multipliers on the pure flexure load and are valid provided that the mechanisms (and the load distributions) for the pure flexure state and any stage under membrane action are identical. Additionally loading magnitudes are provided only in the special case of infinite restraint to a mechanism of infinitely rigid elements. This was referred to at the end of Section 2.3 where it was shown that the rigid-plastic parabola is an envelope to the set of curves for slabs of various stiffnesses associated with the elastic strains in the system. Each of the curves displays a stationary load maximum and is subsequently tangential to the rigid-plastic envelope which occurs simultaneously with membrane force maximum. This was demonstrated in Reference [21]

showing that, whilst the peaks of such curves are not conveniently found, the load at the tangent point is provided directly by a very convenient algebraic expression and may be taken as a reasonably reliable design value for the load somewhat less than the magnitude at the peak. The factor of safety so provided is one which varies according to the nature of the load-deflection curve; the more catastrophic the behaviour the greater the factor of safety.

In the description of membrane action in this current paper, only the one-way strip has been used. The rigid-plastic parabolic unloading curve is modified for the two-way slab. However for all rigid-plastic systems the maximum load factor p at zero displacement is always the same and depends exclusively on the section parameters α, β and γ. The value to the designer is the development of a visual understanding of the effect on slab strength of variations in the parameters that are significant and the realisation of the properties of the system that have little or no effect. A complete graphical construction of load capacity for more general cases of slab will require considerable effort which may not be worth the investment. The required answers may be more conveniently given by hand or machine calculation depending on the stage in the design process. But if suitably simple graphical interpretations can be found the advantages could be considerable.

The benefits of the graphical presentations of plastic lines in elements under plane stress including shear are associated with the mechanisms. In these cases no information is given on the magnitudes of load capacity. Also the progress of any mechanism in these elements is different from that of the flexural slab. The yielding slab, in which the ductility in the yielding reinforcement and the capacity of compressed concrete to support a sustained stress as damage continues, experiences geometric changes and velocity variations during yield. A robust system requiring a continued supply of energy is required for the mechanism to progress. In the case of the above concrete elements under plane stress, the situation of tensile strain ($\varepsilon<0$) or incipient tensile strain ($\dot{\varepsilon} < 0$ at $\varepsilon = 0$) means that the stress state is significantly altered as soon as the mechanism is mobilised. It may be recognised that the presence of aggregate interlock militates against this but its presence defies quantification and will be significantly different for different mix designs, stress combinations, flow vector directions and for different positions on any one line. In these circumstances ductility is lost and flow vectors, determined from the normality rule or from any consideration of the stress state, will not be experienced. Failure is expected to be brittle and from the first occurrence of energy loss the material damage propagates in the manner described by fracture mechanics.

The value of plastic considerations of shear is therefore under question. Calculations of plasticity however are still valuable as providing potential collapse mechanisms. The results may be used to identify reserves of strength offered by restraints to such mechanisms, and provide an opportunity to visualise not only the pattern but also the vector directions of collapse mechanism. Each of these are useful skills for the designer.

5 CONCLUSIONS

The application of plasticity to structural analysis has been welcomed by designers and the appropriate use of either the static or the kinematic theorems often enables design thinking and informed sketching unaided by laborious computation. Prior to the development of machine calculation, graphical methods also provided a convenient and appropriately accurate method of hand analysis whilst drawing up designs.

This paper has identified where the two fields of plasticity and graphics may be combined in a way which assists the designer. Two-dimensional constructions of yield criteria have been illustrated. In the case of the inclusion of membrane action in the upper bound analysis of a reinforced concrete slab, the yield criterion in the space of bending moment and membrane force has been shown to generate the envelope to the slab's load-deflection behaviour and also conveniently to show the effects of variations in section design. This was achieved by the superposition onto the graph of the yield criterion a non-dimensional description of the concrete section given by the reinforcement intensity (Φ) and the cover (h/d). Subsequently, for the case of concrete under plane stress, superposition provides information on the potential flow vectors in a shearing mechanism. In this latter case use is made of the slope of a line in the mechanism and a geometric construction based on the material yield criterion.

In both cases the construction may be used with conventional hand drawing equipment to provide answers of sufficient accuracy for use in design. However this suggestion is not on offer. When analysis requires great accuracy, in say the refinement of a design, it is expected that automated analytical routines will be used. The value here would be the conceptual understanding of the automated processes being used. In the early design stages decisions are being taken on structural

form and component thicknesses fairly repeatedly as different ideas are being tested by sketching. Currently the effect of boundary restraint on the performance of elements is ignored mainly owing to a lack of intuitive awareness. A sufficiently sophisticated piece of software can always be employed, given the time, to provide some answers but a designer is more likely to bare in mind the extra benefits of mechanism constraint if there is some readily available conceptual understanding. The diagrams of this paper may be drawn by hand using the designer's eye to provide proportion and, in the process, give satisfactory ideas of scale when parameters are changed. The work described in this paper, combining geometry and plasticity, is not complete but is offered as an aid to the intuitive understanding that is desirable at the conceptual design stage.

ACKNOWLEDGEMENT

The author thanks Professor James Croll for his very willing help with this paper.

REFERENCES

[1] Calladine, C.R., "An improvement on Magnel's diagram, and an application", *Proceedings of the Institution of Civil Engineers, Structures and Buildings* 159, SB3, 2006, pp 145-152.

[2] Janas, M., "Large plastic deformations of reinforced concrete slabs", *International Journal of Solids and Structures*, 4, 1968, pp 61-74.

[3] Bræstrup, M.W., "Dome effect in RC slabs: rigid-plastic analysis", *Journal of the Structural Division*, ASCE, 106, ST6, 1980, pp. 1237 - 1253.

[4] Morley, C.T., "Yield line theory for reinforced concrete slabs at moderately large deflexions", *Magazine of Concrete Research*, 19, 1967, pp.211-222.

[5] Janas M., "Arching action in elastic-plastic plates", *Journal of Structural Mechanics*, 1, 3, 1973, pp 277-293.

[6] Wood, R.H., *Plastic and Elastic Design of Slabs and Plates*, Thames and Hudson, London, 1961.

[7] Eyre, J.R. & Kemp, K.O., "A graphical solution for predicting the increase in strength of concrete slabs due to membrane action", *Magazine of Concrete Research*, 35, 124, 1983, pp 151-156.

[8] Kemp, K.O., "Yield of a square reinforced concrete slab on simple supports, allowing for membrane forces", *The Structural Engineer,* 45, 7, 1967, **45**, pp. 235-240.

[9] Park, R., "Ultimate strength of rectangular concrete slabs under short-term uniform loading with edges restrained against lateral movement". *Proceedings of the Institution of Civil Engineers*, 28 1964, pp. 125-150.

[10] Christiansen, K.P., "The effect of membrane stresses on the ultimate strength of the interior panel in a reinforced concrete slab", *The Structural Engineer*, 41, 8, 1963, pp. 261-265.

[11] Roberts, E.H., "Load-carrying capacity of slab strips restrained against longitudinal expansion", *Concrete*, 3, 9, 1969, pp.369-378.

[12] Rajendran, S. & Morley, C.T., "A general yield criterion for reinforced concrete slab elements", *Magazine of Concrete Research*, 26, 89, 1974, pp. 212-220

[13] Bræstrup, M.W., "Plastic analysis of shear in reinforced concrete", *Magazine of Concrete Research*, 26, 89, 1974, pp. 221-228.

[14] Nielsen, M.P. & Bræstrup, M.W., "Shear strength of prestressed concrete beams without web reinforcement", *Magazine of Concrete Research*, 30, 104, 1978, pp. 119-128.

[15] Jensen, B.C., "Lines of discontinuity for displacements in the theory of plasticity of plain and reinforced concrete", *Magazine of Concrete Research*, 27, 92, 1975, pp.143-150.

[16] Eyre, J.R. & Campos, E.S., "Upper bounds in the slant shear testing of perfectly plastic joints in concrete", *Magazine of Concrete Research*, 48, 176, 1996, pp. 181-188.

[17] Müller, P., "Plastische Berechnung von Stahlbetonscheiben und-Balken" (Plastic analysis of walls and beams of reinforced concrete), Institut für Baustatik und Konstruktion, ETH Zurich Bericht Nr. 83, Stuttgart, 1978, ps 160.

[18] Marti, P., "Plastic analysis of reinforced concrete shear walls", IABSE colloquium: Plasticity in Reinforced Concrete, Introductory Report, Technical University of Denmark, Copenhagen, 1979, pp. 51-69.

[19] Jensen, J.F., "Plastic solutions for reinforced concrete beams in shear", IABSE colloquium:

Plasticity in Reinforced Concrete, Copenhagen, 1979, Report of the Working Commission, Zurich, 29, 1979, pp. 71-78.

[20] Kemp, K.O. & Al-Safi,M.T., "An upper-bound rigid-plastic solution for the shear failure of concrete beams without shear reinforcement", *Magazine of Concrete Research*, 33, 115, 1981, pp.96-102.

[21] Eyre, J.R., "Direct assessment of safe strengths of R.C. slabs under membrane action", *Journal of Structural Engineering*, ASCE, 123, 10, 1997, pp. 1331 - 1338.